

Ball milling of $\text{Co}_{70}\text{Fe}_8\text{Si}_9\text{B}_{13}$ amorphous ribbon, crystallized ribbon and a mixture of pure crystalline powders

D. OLESZAK, H. MATYJA

Department of Materials Science and Engineering, Warsaw University of Technology, Narbutta 85, 02-524 Warsaw, Poland

$\text{Co}_{70}\text{Fe}_8\text{Si}_9\text{B}_{13}$ amorphous ribbon, crystallized ribbon and a mixture of pure crystalline powders were mechanically alloyed by milling and nanocrystalline structures were obtained. The structural changes were monitored by X-ray diffraction and differential scanning calorimetry measurements. The thermal behaviour on heating the alloys prepared by ball milling was studied and the influence of the high-energy ball milling on the resulting phases was found.

1. Introduction

At present there is a considerable interest in the formation of amorphous and nanocrystalline phases in magnetic alloy systems. It is known that Co- and Fe-base amorphous alloys exhibit superior soft magnetic properties. High-energy ball milling (mechanical alloying by milling) has recently become an effective method for the preparation of powders of magnetic metal-metalloid alloys. This technique has been successfully applied to obtain amorphous or nanocrystalline Fe-Si-B alloys from pure elemental powders [1–3]. There are only a few reports on the mechanical milling of crystallized ribbons [4,5]. Powders of amorphous alloys can also be prepared by milling metallic glass ribbons produced by the melt-spinning process. However, changes in their properties and partial or full crystallization usually occur during the milling [6,7].

In this paper the progress of disordering by ball milling/mechanical alloying of $\text{Co}_{70}\text{Fe}_8\text{Si}_9\text{B}_{13}$ crystallized ribbon and a mixture of pure crystalline powders is presented as monitored by X-ray diffraction and differential scanning calorimetry (DSC). The results of the influence of high-energy ball milling on the crystallization of $\text{Co}_{70}\text{Fe}_8\text{Si}_9\text{B}_{13}$ amorphous ribbon are reported as well.

2. Experimental procedure

The experimental procedure consisted of the following three separate stages:

- (a) casting of amorphous $\text{Co}_{70}\text{Fe}_8\text{Si}_9\text{B}_{13}$ ribbon,
- (b) crystallization of the ribbon at elevated temperature, and
- (c) ball milling (BM) processes performed for amorphous ribbon, crystallized ribbon and a mixture of pure crystalline powders.

$\text{Co}_{70}\text{Fe}_8\text{Si}_9\text{B}_{13}$ metallic glass ribbons were obtained by the melt-spinning technique. The ribbon width and thickness were about 9 mm and 30 μm , respectively. The ribbon was fully crystallized by vacuum annealing at 900 K for 0.5 h.

Amorphous ribbon prior to ball milling was low-temperature vacuum-annealed at 670 K for 0.5 h to make it brittle, preserving its amorphous structure. Both amorphous and crystallized initially broken ribbons were used as starting materials for the ball milling processes. A mixture of crystalline powders (purity 99.8%) of the desired atomic composition was subjected to milling as well.

The ball milling processes were conducted in a vibrational-type mill. Stainless steel vials and balls were used. The weight ratio of balls to milled material was 5:1.

The structure of the starting materials and the ball-milled samples of different stages of milling and after completion of the process was monitored by a Philips PM 8000 X-ray diffractometer with CoK_α radiation ($\lambda = 0.179021$ nm).

Calorimetric measurements were carried out in a Perkin Elmer DSC-2 unit within the temperature range 320–1000 K at a continuous heating rate of 40 K min^{-1} .

3. Results

3.1. Amorphous ribbon

In Fig. 1 the X-ray patterns of samples subjected to milling for the quoted times are shown. For comparison the X-ray traces relevant to the as-quenched and low-temperature annealed ribbons (the last one being used as a starting material for the ball milling process) are presented as well. No significant changes are observable in the patterns registered after increasing milling time. One can consider that the material

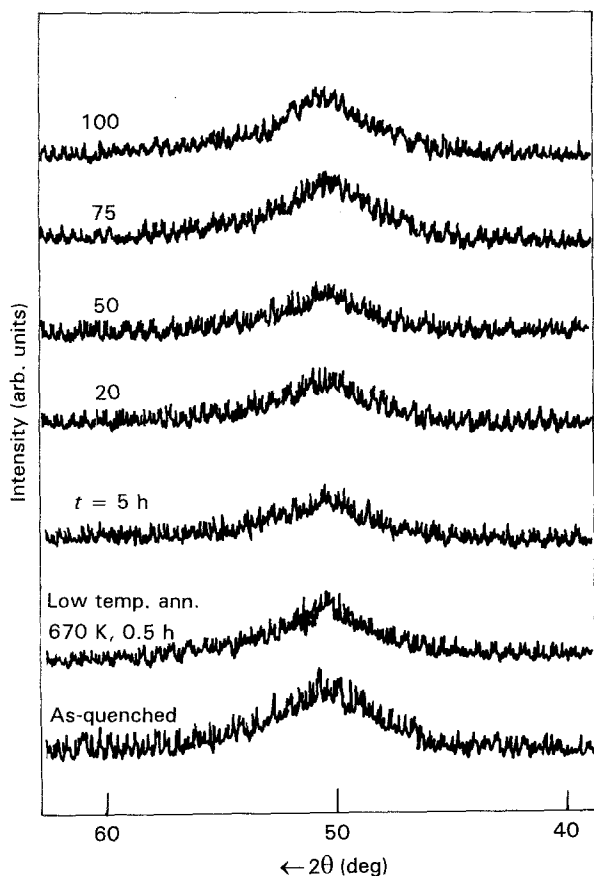


Figure 1 X-ray patterns of amorphous ribbon subjected to milling for different times.

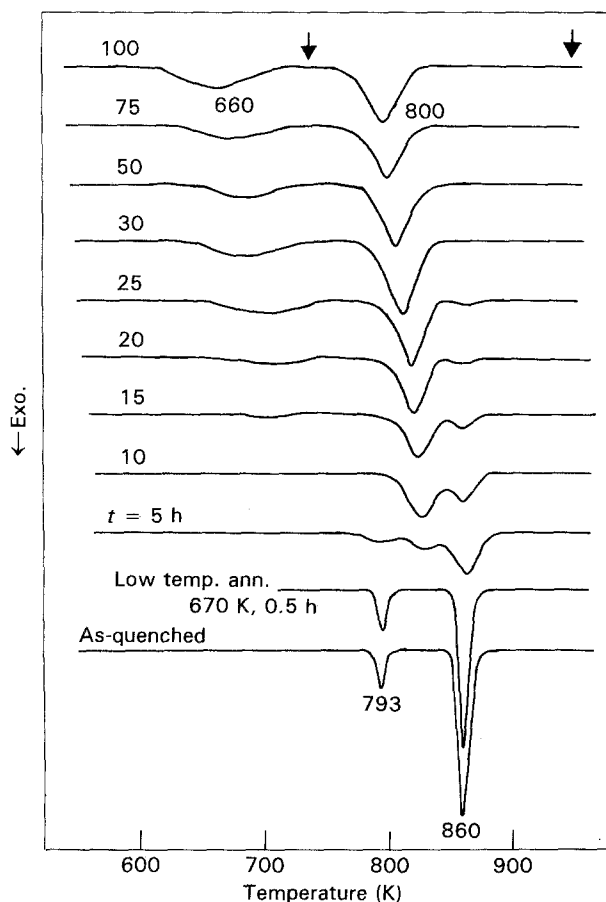


Figure 2 DSC curves taken for amorphous ribbon at different milling times.

remains amorphous. Detailed studies show, however, some changes in the width of the registered line. After 100 h of ball milling the full width at half maximum (FWHM) becomes smaller than for the starting amorphous ribbon.

The sequence of DSC curves taken after different milling times is presented in Fig. 2. DSC curves recorded for as-quenched and low-temperature annealed ribbons are shown as well. Comparison of these two curves confirms the X-ray results that low-temperature annealing performed on the ribbon to make it brittle prior to ball milling did not cause its crystallization. The characteristic temperatures for annealed ribbon are the same as for the as-quenched one. Two exothermic peaks registered at temperatures $T_{p1} = 793$ K and $T_{p2} = 860$ K are attributed to the crystallization processes of Co-base solid solution and Co_2B phases, respectively [8].

However, one can notice dramatic changes in the DSC curves with increasing milling time. The two initial exothermic peaks disappear after 10 and 30 h of ball milling, respectively. Simultaneously, after 5 h of BM a new exothermic effect appears, becoming the main peak after 100 h of the process. In addition a low-temperature exothermic effect is registered, starting from 15 h of milling. All peaks (appearing and vanishing) exhibit a tendency to shift into the lower-temperature range with increasing milling time.

Thus the starting DSC curve transforms upon milling into a curve also showing two exothermic effects at temperatures $T_{p1} = 660$ K and $T_{p2} = 800$ K. However, these effects are diffuse and occur in a lower temperature range than for starting amorphous ribbon subjected to the ball milling process. Comparison of Figs 1 and 2 indicates that DSC is more sensitive than X-ray diffraction for identifying the character of the sample.

In order to identify by X-ray diffraction the phase changes with temperature, the heating of 100 h BM samples was interrupted at two different temperatures during a DSC run, namely at 740 and 950 K (marked by arrows in Fig. 2). Isothermal vacuum annealing for 1 h at the same temperatures as mentioned above was performed as well.

The X-ray patterns obtained for the samples heat-treated at the two temperatures given above are shown in Figs 3 and 4, respectively. After continuously heating the sample up to 740 K one peak is visible at the angle position corresponding to the diffuse maximum registered after 100 h of BM. Assuming a nanocrystalline structure of the sample, the average crystallite size estimated by Scherrer's formula [9] is 14 nm. A similar result is observed after isothermal annealing at the same temperature, although the Co-base solid solution line appears in addition.

The X-ray spectra recorded after continuously heating the samples up to 950 K and isothermal annealing at this temperature (Fig. 4) reveal peaks corresponding to Co-base solid solution and Co_2B phases.

Thus the first low-temperature DSC exothermic effect is connected with the formation of nanocrystalline structure. The second peak corresponds to the

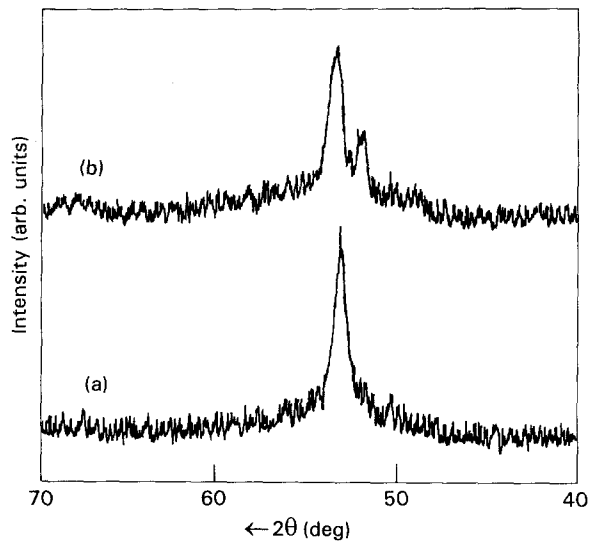


Figure 3 X-ray diffraction spectra of amorphous ribbon after 100 h of ball milling and (a) continuous heating up to 740 K or (b) isothermal annealing at 740 K for 1 h.

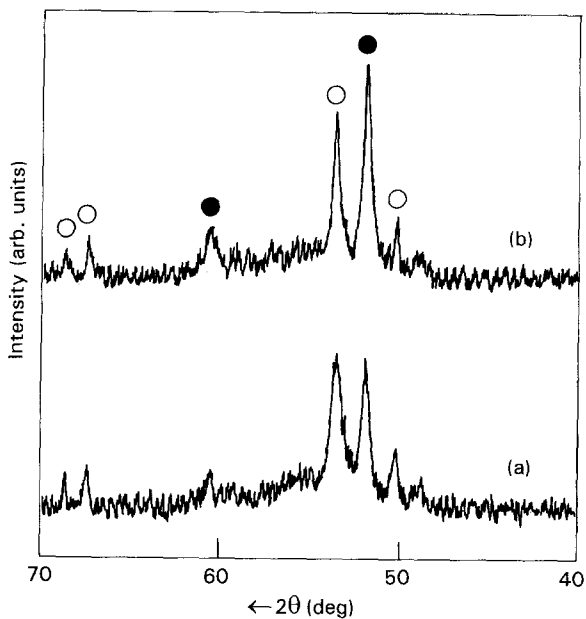


Figure 4 X-ray results for 100 h ball-milled amorphous ribbon (a) continuously heated up to 950 K or (b) isothermally annealed at 950 K for 1 h; (●) f.c.c. Co-base solid solution, (○) Co_2B .

simultaneous development of Co-base solid solution and boride phases.

3.2. Crystallized ribbon

The X-ray diffraction spectra obtained for ball-milled and previously crystallized ribbon at selected time intervals are presented in Fig. 5. The X-ray pattern relevant to the starting crystallized ribbon is also shown; all peaks were identified as belonging to Co-base solid solution, Co_2B and Co_2Si phases. A single, markedly broadened peak is already observed after 20 h of the process. This peak undergoes only further minor evolution. The average crystallite size calculated from Scherrer's formula for the final pattern obtained after 100 h of BM is 4 nm.

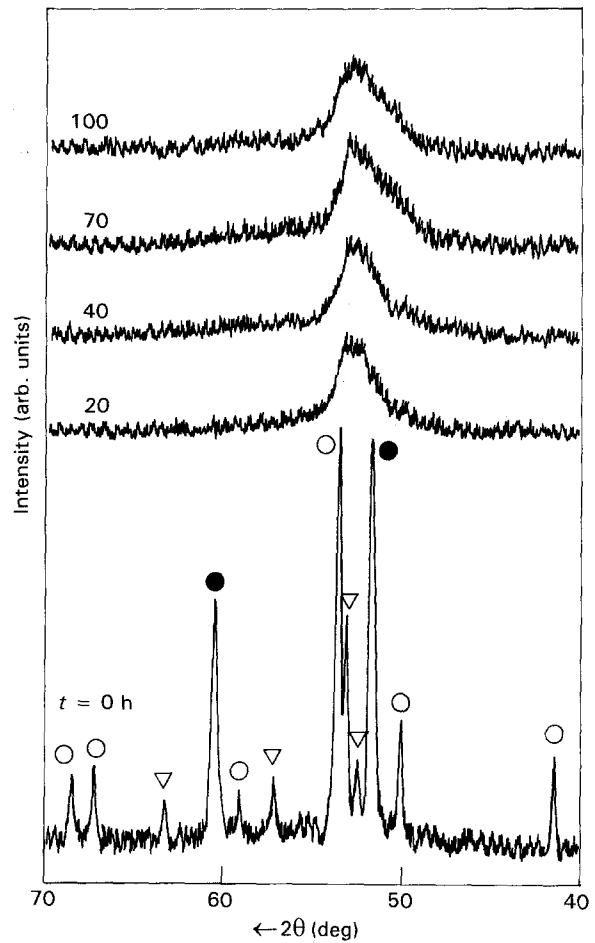


Figure 5 X-ray patterns for crystallized ribbon subjected to mechanical milling for different times: (●) f.c.c. Co-base solid solution, (○) Co_2B , (▽) Co_2Si .

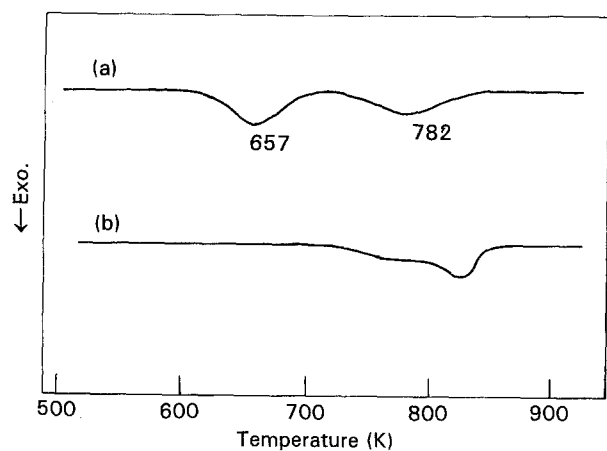


Figure 6 DSC traces registered after 100 h of ball milling of (a) crystallized ribbon and (b) a mixture of pure elemental powders.

Structural changes during the milling were followed by DSC measurements as well. For milling times shorter than 40 h no heat effects are visible in the registered curves. This behaviour is surprising, taking into account the X-ray results and the sensitivity of calorimetric measurements to structural changes. However, starting from 50 h of BM two diffuse exothermic peaks appear in the DSC curve. These peaks remain almost unchanged with increasing milling time. The final DSC curve taken after 100 h of ball milling is shown in Fig. 6 (upper curve (a)). The peak

temperatures ($T_{p1} = 657 \text{ K}$, $T_{p2} = 782 \text{ K}$) as well as the shape of the curve are close to the ones obtained for 100 h ball-milled amorphous ribbon.

In order to explain the DSC results for crystallized 100 h BM ribbon the same heat-treatment procedure as for the milled amorphous ribbon was applied. Continuous heating up to 700 and 950 K during DSC runs and 1 h isothermal annealing at the same temperatures were performed.

The X-ray patterns of the samples heat-treated at both temperatures are shown in Figs 7 and 8, respectively. As can be seen, both patterns for the lower temperature applied reveal the nanocrystalline character of the samples. The average crystallite size is 6 nm for the sample continuously heated up to 700 K and 23 nm after isothermal annealing at the same temperature. A fully crystalline pattern develops only when high-temperature isothermal annealing is applied (upper spectrum (b) in Fig. 8). However, the phase composition is different from that of the starting crystallized ribbon. The two strongest registered diffraction lines correspond to the Co_2Si phase. Other lines of this phase also appear as well as those of Co_3B boride. The intensity of Co-base solid solution peaks is markedly reduced. This testifies that the milling of crystallized ribbon results in the easier formation of silicide and boride phases during subsequent heat treatment.

3.3. Mixture of pure crystalline powders

The changes in the X-ray diffraction pattern of an elemental powder mixture with milling time are shown in Fig. 9. The spectrum of the sample subjected to 25 h of mechanical alloying reveals only a broad diffraction line, indicating that the mixture of crystalline powders has transformed into a nanocrystalline alloy. Further milling up to 100 h causes line broadening only. The

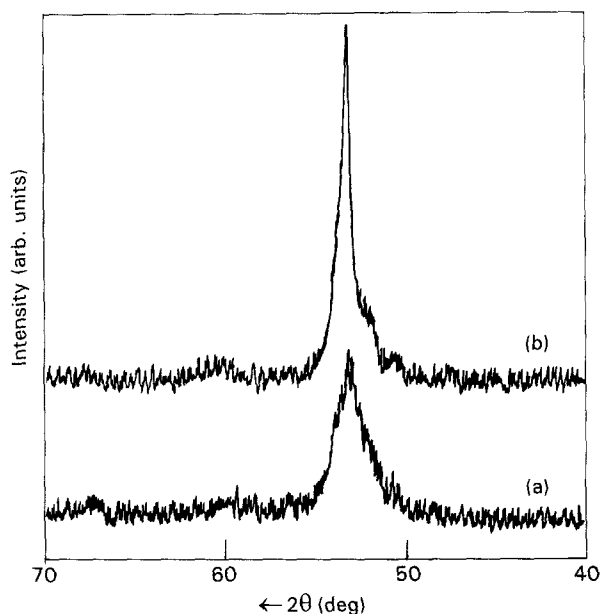


Figure 7 X-ray diffraction patterns of 100 h ball-milled crystallized ribbon (a) continuously heated up to 700 K or (b) isothermally annealed at 700 K for 1 h.

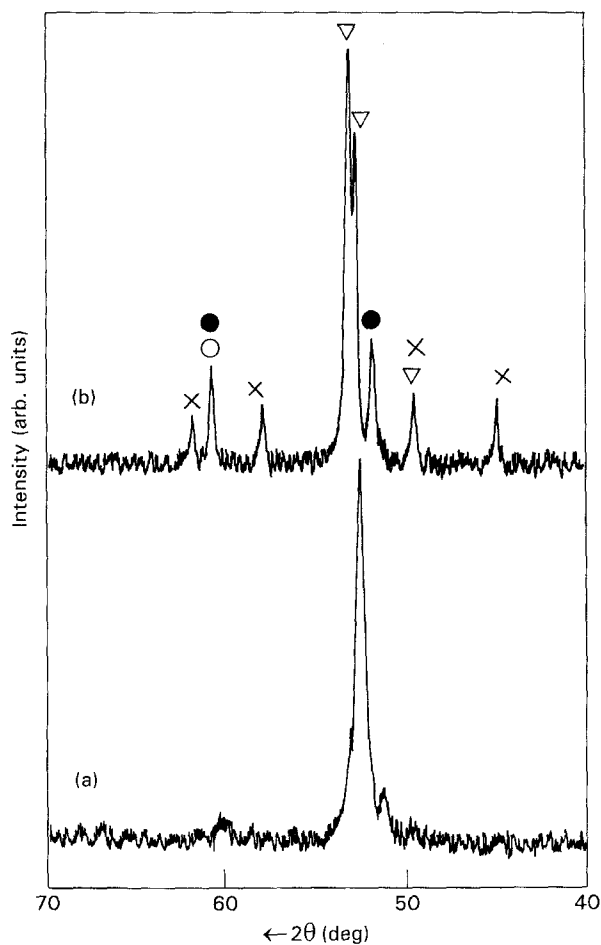


Figure 8 X-ray patterns for 100 h ball-milled crystallized ribbon after (a) continuous heating up to 950 K (b) isothermal annealing at the same temperature for 1 h: (●) f.c.c. Co-base solid solution, (▽) Co_2Si , (○) Co_2B , (×) Co_3B .

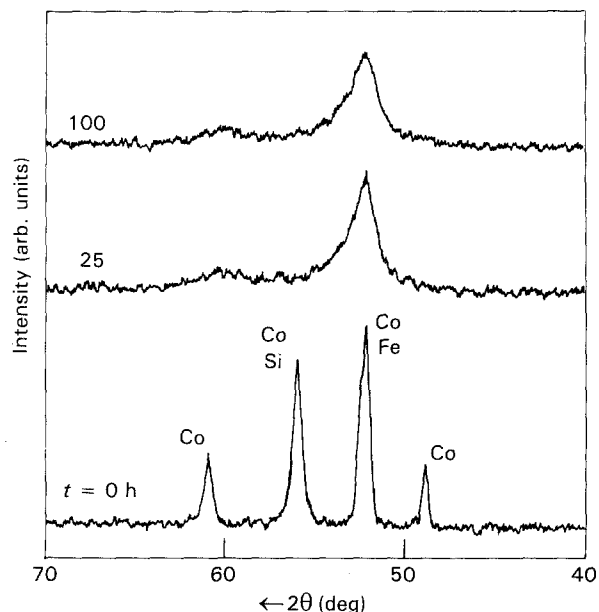


Figure 9 X-ray spectra obtained for a mixture of pure elemental powders mechanically alloyed for different times.

mean crystallite sizes calculated from Scherrer's formula are 14 and 11 nm after 25 and 100 h of mechanical alloying, respectively.

The DSC curve taken during continuous heating of the 100 h milled sample is shown in Fig. 6 (lower curve

(b). Broad exothermic reactions occur in the temperature range 700–850 K.

The X-ray diffraction pattern of the sample after heating in the DSC up to 950 K reveals a decrease of the line width and no additional peaks appear. The calculated crystallite size after heating is 22 nm. Thus the diffuse exothermic DSC effects are attributed to crystallite growth of the nanocrystalline alloy.

4. Discussion

A comparison of the results obtained for mechanically milled amorphous and crystallized ribbons testifies that very similar final structures have been produced after 100 h of ball milling. The average crystallite size for milled crystallized ribbon has been estimated to be 4 nm, but the existence of an amorphous phase is not excluded. On the other hand, the change in the FWHM of the diffraction pattern registered for 100 h BM amorphous ribbon suggests that the crystallization process has started. One can conclude that the applied milling energy has not been sufficient for full crystallization of amorphous ribbon and full reamorphization in the case of ball-milled crystallized ribbon. On the other hand, taking into account that the ribbon was crystallized before the milling by annealing at a temperature well above the crystallization temperature determined by DSC, one can conclude that the grain size of the starting material exceeded the diffusion range necessary for full reamorphization during the ball milling process. It has been shown that the grain size of the starting material influences the possibility of reamorphization of ball-milled crystallized ribbon [4].

The DSC results also confirm the similarities of the final structures obtained. The characteristic temperatures of both exothermic effects and the shapes of the curves are very close. The first low-temperature exothermic effect has proved to be connected with the nanocrystal growth process. The second DSC peak corresponds to the formation of Co-base solid solution and boride and silicide phases. Ball milling forces the simultaneous development of all phases during the DSC heating, although for melt-spun ribbon these processes are well separated and occur in a higher temperature range.

A significant difference has been found in the phase composition after high-temperature heat-treatment of the samples. High-energy ball milling strongly influences the resulting phases. For ball-milled amorphous ribbon the phase composition after isothermal annealing at 950 K for 1 h is very similar to that of the crystallized amorphous ribbon. In contrast, ball-milled and heat-treated crystallized ribbon reveals the domination of the Co-rich phases Co_2Si and Co_3B ; in addition, Co-base solid solution occurs. This result testifies to the easier formation of silicide and boride phases during heat-treatment following the milling of crystallized ribbon. A similar result has been published recently for $\text{Ni}_{78}\text{Si}_{10}\text{B}_{12}$ metallic glass ribbon subjected to ball milling [10].

The nanocrystalline structure obtained after mechanical alloying of the mixture of pure elements reveals a higher thermal stability than for the two ball milled-ribbons. After high-temperature heat-treatment only grain growth is observed and a fully crystalline structure is not developed.

References

1. S. SURINACH, M. D. BARO, J. SEGURA, M. T. CLAVAGUERA-MORA and N. CLAVAGUERA, *Mater. Sci. Eng.* **A134** (1991) 1368.
2. A. CALKA, A. P. RADLINSKI and R. SHANKS, *ibid.* **A133** (1991) 555.
3. T. OGASAWARA, A. INOUE and T. MASUMOTO, *ibid.* **A134** (1991) 1338.
4. A. CALKA, A. P. POGANY, R. SHANKS and H. ENGELMAN, *ibid.* **A128** (1990) 107.
5. H. MATYJA, D. OLESZAK and J. LATUCH, *Mater. Sci. Forum* **88** (1992) 297.
6. M. L. TRUDEAU, R. SCHULZ, D. DUSSAULT and A. VAN NESTE, *Phys. Rev. Lett.* **64** (1990) 99.
7. HAN-RYONG PAK, JING CHU, R. J. DEANGELIS and K. OKAZAKI, *Mater. Sci. Eng.* **A118** (1989) 147.
8. A. ZALUSKA and H. MATYJA, *Acta Magn. Suppl.*, (1987) 325.
9. B. CULLITY, "Elements of X-ray Diffraction" (Addison-Wesley, London, 1978) p. 447.
10. I. A. TOMILIN, T. J. MOCHALOVA and S. D. KALOSH-KIN, *Mater. Sci. Forum* **88** (1992) 289.

Received 13 October 1992
and accepted 21 September 1993